Fish and Shellfish Immunology 89 (2019) 486–497

Contents lists available at ScienceDirect

Fish and Shellfish Immunology

journal homepage: www.elsevier.com/locate/fsi

Full length article

Characterization of a CD59 in orange-spotted grouper (*Epinephelus coioides*)

Sheng-Wei Luo[a,b,1], Wei Wei[a,1], Ping Yang[a], Chu-Min Lai[a], Qing-jian Liang[a], Yuan Liu[a], Wei-Na Wang[a,*]

[a] Guangzhou Key Laboratory of Subtropical Biodiversity and Biomonitoring, Guangdong Provincial Key Laboratory for Healthy and Safe Aquaculture, College of Life Science, South China Normal University, Guangzhou, 510631, PR China
[b] State Key Laboratory of Developmental Biology of Freshwater Fish, College of Life Science, Hunan Normal University, Changsha, 410081, PR China

ARTICLE INFO

Keywords:
Epinephelus coioides
CD59
Gene expression
Vibrio alginolyticus

ABSTRACT

CD59, a multifunctional glycoprotein, not only plays a regulatory role in complement cascades, but also participates in modulation of teleostean immunity. In this study, full length sequence of EcCD59 was obtained, comprising a 5′UTR of 163 bp, an ORF of 354 bp and a 3′UTR of 559 bp. EcCD59 gene encoded a polypeptide of 117 amino acids. Tissue-specific analysis revealed that the highest expression of EcCD59 mRNA was observed in muscle. *Vibrio alginolyticus* challenge can significantly increase EcCD59 mRNA expression in liver, kidney and spleen. EcCD59 distribution was detected by a combined approach using GFP-overexpression, immunofluorescence and ELISA assay, indicating that EcCD59 may be predominantly aggregated in cellular membrane. Both EcCD59 and EcCD59delGPI can directly bind to *V. alginolyticus* and decrease the *in vitro* growth of *V. alginolyticus*. Additionally, vibrio injection experiment indicated that the binding of EcCD59 or EcCD59delGPI to *V. alginolyticus* can restrict its growth rate *in vivo*. In this study, we found that EcCD59 may be involved in immune defense against vibrio infection in a complement-independent manner.

1. Introduction

In mammals, cell killing mechanism is playing a key role in immune defense system and exhibits a cytotoxic effect on invading pathogens, infected tissues and malignant cells [1]. Accumulating evidences demonstrate that macrophage-activating cytokines can exhibit a regulatory effect on complement system [2], thus regulating the processes of phagocytosis [3], inducing superoxide production [4] as well as bridging innate immunity with adaptive immune response [5]. As is well known, three major complement pathways in complement system can generate active complement fragments, then mediating lysis process of invading pathogens by forming perforin-like proteins or membrane attack complexes (MAC) [6]. Recent findings indicate that pretreatment of LPS can effectively activate mammalian complement system, which can increase phagocytic activity and confer protection against bacterial challenge, but destroyed complement cascades can significantly abolish *in vivo* clearance activity of invading pathogens, causing an elevated susceptibility to bacterial infection and leading to an increasing prevalence of immune complex diseases [7,8].

CD59, a small and widely distributed glycoprotein, belongs to leukocyte antigen 6 (Ly-6) family and shares a similar “three finger” architecture with 4–5 disulfide bonds formed by conserved cysteine residues [9]. Besides, CD59 also contains a GPI anchor located at the C-terminal end, which can bind to cell membrane phospholipids [10]. Despite the members of Ly-6 family contains a conserved motif “CCX-XXXCN”, only CD59 can exhibit a regulatory effect on the complement system and its disulfide structures are involved in complement inhibition [11,12]. As is well known, complement signaling is converged on MAC formation, but CD59 is playing a negative regulatory role in complement pathways, which can inhibit the incorporation of C9 into membrane-bound complex of C5b-9 assembly by directly binding to C8α or C9b [13,14]. In addition, CD59 also serves as a multifunctional signaling molecule that can participate in T cell activation [15], insulin secretion [16] and tumor growth [17].

Evidences are emerging that innate immune defense system in invertebrate possesses various pathogen-recognizing systems, whereas it is only a fundamental defense in teleost [18]. For instances, teleost contains a developed complement system and complement proteins show a high similarity to their counterparts in mammals [19–21]. Although most studies focus on function of mammalian genes synchronizing innate immunity with adaptive immune responses, only a few reports study on the architecture and expression of teleostean

* Corresponding author. College of Life Science, South China Normal University, Guangzhou, 510631, PR China
E-mail addresses: weina63@aliyun.com, wangwn@scnu.edu.cn (W.-N. Wang).
[1] These authors contributed equally to this work.

https://doi.org/10.1016/j.fsi.2019.04.020
Received 12 September 2018; Received in revised form 4 April 2019; Accepted 6 April 2019
Available online 11 April 2019

complement genes or complement-regulatory genes. In recent years, teleostean CD59s are only identified in zebrafish [11], Nile tilapia [22], large yellow croaker [23] and Tongue sole [24]. Additionally, the data on expression levels of grouper CD59 under vibrio challenge and its function in immunity are also limited.

Orange-spotted grouper (*Epinephelus coioides*) is one of the most important economic marine fish, mainly distributed in tropical and subtropical water areas. However, the emergence of global climate anomaly may be one of the abnormal phenomena and exhibits a lingering effect in the expansion of seafood-borne or water-borne pathogenic diseases [25,26], thereby posing a significant threat to the survival of aquatic organisms [27]. Recently, stressors may also exert an adverse effect on grouper immunity [28,29]. *Vibrio alginolyticus* possessing a highly toxic extracellular product is one of the most serious threats to survival of groupers [30]. In general, the increasing vibrio population in an estuarine environment may be highly associated with enhanced level of fecal pollution in water. Vibrio population may significantly increase to approximately 1.3×10^7 CFU/g sediment during a high-intensity aquaculture process [31]. Additionally, TonB/ExbB/ExbD complex in vibrio strain can exhibit a regulatory effect on the process of iron uptake and metabolism, thus rendering invading vibrio more resistant to a microenvironmental condition of limited iron availability [32]. Recent studies indicate that an isolated vibrio strain EMI2KL can increase to LD_{50} value of approximately 2.57×10^7 CFU/g grouper body weight with a higher virulence activity [33]. Thus, the study on the immune response to vibrio infection in grouper may be propitious to the sustainable development of aquaculture.

In this study, the aims were to characterize the full-length EcCD59 cDNA in orange-spotted grouper and measure tissue distribution of EcCD59 mRNA. We also assessed the effect of *V. alginolyticus* challenge on the expression patterns of EcCD59 mRNA in various immune tissues. To further characterize its functionality, we also studied binding activity of EcCD59 to vibrio and its potential effect on *V. alginolyticus* growth.

2. Materials and methods

2.1. Animals

Orange-spotted groupers with average length 10.70 ± 0.33 cm and average weight 12.50 ± 0.38 g, were obtained from an aquaculture farm in Leizhou (Guangdong, China). Groupers were acclimatized in 70 × 65 × 65 cm plastic aquarium (25 fishes/aquarium) with the diluted seawater (15‰ salinity, pH 8.0, 25 ± 1 °C) for two weeks. The groupers were fed with the commercial diet twice daily till 24 h before challenge experiment.

2.2. Gene cloning

According to the highly conserved domains of EcCD59 sequence from other species in GenBank database (http://www.ncbi.nlm.nih.gov/genbank/), ORF sequences of EcCD59 were obtained by touchdown PCR using the primers shown in Tab.1, and the liver cDNA of orange-spotted grouper was used as template. Then, 5′ and 3’ rapid amplification of cDNA ends (RACE) were performed to obtain full-length sequences of EcCD59 by using the BD SMART RACE cDNA reaction kit (BD Bioscience Clontech, CA, USA). Gene-specific primers and nested primers were shown in Table 1.

2.3. Sequence alignment and evolutionary analyses

Both nucleotide sequence and amino acid sequence of EcCD59 were analyzed on the NCBI blast program (http://www.ncbi.nlm.nih.gov/blast/Blast.cgi). Conserved domains of EcCD59 sequence were predicted by motif scan analysis program (http://myhits.isb-sib.ch/cgi-bin/motif_scan). EcCD59 amino acid sequence analysis was performed by using ExPASy tools (http://expasy.org/tools/). Signaling peptide of deduced EcCD59 amino acid sequence was predicted by using SignalP 4.1 server (http://www.cbs.dtu.dk/services/SignalP/). Multiple sequence alignments of CD59 amino acid sequences were constructed by using ClustalW program and Genedoc program. Phylogenetic tree was constructed in accord with amino acid sequences of CD59s by MEGA 6.0, using neighbor-joining method with 1000 bootstrap replications.

2.4. Immune challenge experiment with Vibrio alginolyticus

Strain of *V. alginolyticus* was cultured in seawater medium (1‰ yeast extract, 3‰ beef extract, 5‰ peptone, pH 7.2) for 24 h at 28 °C. Seawater medium was centrifuged at 10000 × *g* for 15 min at 4 °C, and resuspended in 1 × PBS (phosphate-buffered saline, pH 7.3). Based on previous studies on teleostean immune experiment, the concentration of *V. alginolyticus* was adjusted to 1×10^7 CFU ml^{-1} before the immune challenge experiment [34]. In lab, orange-spotted groupers were acclimated into separated plastic aquarium with diluted seawater (15‰ salinity, pH 8.0, 25 ± 1 °C) for 24 h before vibrio challenge experiments. Vibrio challenge was performed by intraperitoneal injection of 100 μl suspension of *V. alginolyticus* in PBS. In addition, the groupers injected with 100 μl sterile PBS were used as the control group. Each group was composed of six groupers, and each treatment contained three replicates under the same conditions. Tissues were isolated at 0, 6, 12, 24 and 36 h post-injection, immediately frozen in liquid nitrogen and preserved in −80 °C.

2.5. RNA extraction and cDNA synthesis

According to the phenol-chloroform method, total RNA was extracted from isolated samples by using Trizol Reagent (Invitrogen, USA) [35]. Concentration and purity quotient of RNA was determined by measurement of 260 nm absorbance and 260/280 nm absorbance, respectively. Integrity of total RNA was determined by 1% agarose gel electrophoresis, then purified total RNA of each group was used to synthesized cDNA. 1000 ng of total RNA was added and incubated with Dnase I (Invitrogen, USA), and immediately used to synthesize cDNA by using oligo-d(T)18 primers and Revert Aid™ M-MuLV Reverse Transcriptase Kit (MBI Fermentas, USA) following protocols of the manufacturer.

2.6. qRT-PCR assay

Tissue-specific expression and vibrio-stimulated expression of EcCD59 were detected by qRT-PCR, respectively. Differential expression analyses of EcCD59 (MF678852) were measured by using ABI 7500 Real-Time PCR system (Applied Biosystems, USA). Besides, the expression of 18S rRNA was measured and used as internal control to normalize results of qRT-PCR analyses. Both primers of target genes and 18S rRNA for qRT-PCR were shown in Tab 1, respectively. qRT-PCR was performed in a volume of 20 μl, including 0.8 μl of each primer (10 μM), 6.0 μl of PCR-grade water, 2 μl of 1:10 diluted cDNA, 0.4 μl of ROX Reference Dye (50 ×) and 10 μl of SYBR premix Ex Taq™ II (Perfect Real Time) (TaKaRa, Dalian, China). The program contained 1 cycle of 95 °C for 30s, 40 cycles of 95 °C for 15 s, 60 °C for 35 s, followed by 1 cycle of 95 °C for 30s, 60 °C for 60s. At the end of qRT-PCR amplified reactions, melting curve analysis was implemented to confirm credibility of each qRT-PCR analysis. cDNA of each sample isolated from six groupers in each treatment was detected by qRT-PCR analysis. Each sample was analyzed in triplicate to certify the repetitiveness and credibility of experimental results. qRT-PCR results were measured by using 7500 software (Applied Biosystems, USA) with $2^{-\triangle\triangle Ct}$ methods [36].

Table 1
The primer sequences used in this study.

Primer names	Sequence direction (5′ → 3′)	Use
EcCD59-F	ATGAAGCACTCCCTGGGGAT	clone
EcCD59-R	TCAGTGGATGCACCACCACA	clone
EcCD59-5gsp	GCAGCACTTGAAGGTGAAACTGGAGA	5′-race
EcCD59-3gsp	CCGACTGTCCCAAATGTTCCCC	3′-race
EcCD59-5np	TGTGAGACAGGCATCGTCATAGC	5′-race
EcCD59-3np	CGATGTCTGTGATTGGTCTTCTGGC	3′-race
EcCD59delGPI-F	ATGAAGCACTCCCTGGGGAT	truncation
EcCD59delGPI-R	CATCGATGCAGAGGAGGGGG	truncation
pGEX-EcCD59(delGPI)—F	CCGGAATTCCGATGAAGCACTCCCTGGGGAT	vector
pGEX-EcCD59-R	CCGCTCGAGC TCAGTGGATGCACCACCACA	vector
pGEX-EcCD59delGPI-R	CCGCTCGAGCTTACATCGATGCAGAGGAGGG	vector
pEGFP-EcCD59(delGPI)—F	CCGGAATTCGATGAAGCACTCCCTGGGGAT	vector
pEGFP-EcCD59-R	CGCGGATCCGTGGATGCACCACCACATGA	vector
pEGFP-EcCD59delGPI-R	CGCGGATCCCATCGATGCAGAGGAGGGGG	vector
RT-18S-F	CCTGAGAAACGGCTACCACATCC	qPCR
RT-18S-R	AGCAACTTTAGTATACGCTATTGGAG	qPCR
RT-EcCD59-F	TGTCCCAAATGTTCCCCCAG	qPCR
RT-EcCD59-R	GGATGCACCACCACATGACT	qPCR
RT-gyrB-F	TCAGAGAAAGTTGAGCTAACGATT	qPCR
RT-gyrB-R	CATCGTCGCCTGAAGTCGCT	qPCR
RT-GAPDH-F	GTAAGCTGTGGAGGGATGGC	qPCR
RT-GAPDH-R	GGACTGTCAGGTCAACCACG	qPCR

2.7. Plasmid construction

To investigate EcCD59's function, we cloned a full-length sequence of EcCD59 and amplify GPI domain deleted EcCD59 (EcCD59delGPI) by using the primers shown in Tab 1. Following double digestion reaction, the above sequences were ligated to expression plasmids such as pGEX4T-2 and pEGFP-N3. All recombinant plasmids were confirmed by sequencing for further studies.

2.8. Subcellular localization

Subcellular localization of EcCD59 and EcCD59delGPI was performed as previously described [37]. In brief, Hela cells were seeded in 24-well plates and incubated for 18 h. According to manufacturer's protocols (Invitrogen), cell transfection was performed by using Lipofectamine 3000 reagent. In brief, Lipofectamine 3000 and pEGFP-N3, pEGFP-N3-EcCD59 or pEGFP-N3-EcCD59delGPI plasmid were mixed for 10 min before cell transfection. Cells were incubated with the mixture at 37 °C for 6 h, and cultured with fresh medium. After that, cells were washed with PBS, fixed with 4% paraformaldehyde and stained with DAPI. Fluorescence signaling was detected by using a fluorescence microscope (Nikon). The experiment was performed in triplicate.

2.9. Immunofluorescence

To investigate CD59 distribution in liver tissue, immunofluorescence assay was performed as previously described [38]. Briefly, following antigen retrieval, paraffin-embedded liver sections were incubated with 1:100 diluted anti-CD59 primary antibody (Abcam) overnight at 4 °C. After washing, the slides were incubated with 1:500 diluted FITC-conjugated IgG secondary antibody (Abcam) at room temperature for 1 h. Following washing 3 times with PBS, the slides were incubated with DAPI or membrane probe $DiIC_{18}(3)$ (DiI) for another 20 min, respectively. The fluorescence signaling was detected by using a fluorescence microscope (Nikon). The experiment was performed in triplicate.

2.10. Detection of EcCD59 in nucleus, cytoplasm and membrane by ELISA assay

Nuclear proteins, cytoplasmic proteins and membrane proteins in liver tissue were isolated by using nuclear and cytoplasmic protein extraction kit (Beyotime Institute of Biotechnology, Jiangsu, China) and membrane protein extraction kit (Sangon Biotech, Shanghai, China). Then, the concentration of isolated proteins was determined by using BCA method. After that, ELISA assay was performed by using a CD59 ELISA kit (Sino Biological, Beijing, China). In brief, 1:1000 diluted anti-CD59 primary antibody in a volume of 200 μl per well was coated in a 96-well plate at 4 °C overnight, then was incubated at 37 °C for another 1 h. Following washing 3 times, the plate was blocked and incubated with various concentrations of liver nuclear proteins, cytoplasmic proteins and membrane proteins at room temperature for 2 h, followed by the incubation of HRP-conjugated CD59 antibody. Then, 200 μl of TMB in substrate buffer was added and incubated in dark for 30 min. Until the color was developed, 2 M H_2SO_4 was added. The absorbance at 450 nm was determined by a microplate reader [39]. In this study, PBS group was served as negative control and binding index was calculated as follows: OD_{450} nm absorption in text group/OD_{450} nm absorption in negative control group (n = 3).

2.11. Prokaryotic expression, purification and western blotting of EcCD59 and EcCD59delGPI

To obtain purified CD59 and EcCD59delGPI fusion proteins, the protocols of recombinant protein expression and purification were performed as previously described [40]. In brief, the above pGEX4T-2-EcCD59 plasmid or pGEX4T-2-EcCD59delGPI plasmid was transformed into *E. coli* BL21 (DE3) competent cells for protein expression, respectively. The bacterium clone with the corrected plasmid insertion was cultured in LB medium containing 100 μg/ml ampicillin at 37 °C with vigorous shaking until OD_{600} reached approximately 0.8. After that, IPTG was added to the above culture medium to a final concentration of 1 mM for another 4 h induction. Then, cells were harvested by centrifugation at 8000*g* for 15 min and resuspended for sonication, followed by the protein purification by using GST resin (Millipore). The concentration of recombinant fusion proteins was determined by using Bradford's method. Finally, the purified proteins were loaded on 12% SDS-PAGE gel, separated electrophoretically and visualized by staining with coomassie blue R250. According to our previous studies, western blotting was performed. Briefly, the above purified recombinant proteins were loaded on 12% SDS-PAGE gels and electrophoretically separated. SDS-PAGE gels were washed in TBST (50 mM Tris-Hcl pH 8.0, 150 mM NaCl and 0.05% Tween-20) for 5 min, and then the separated

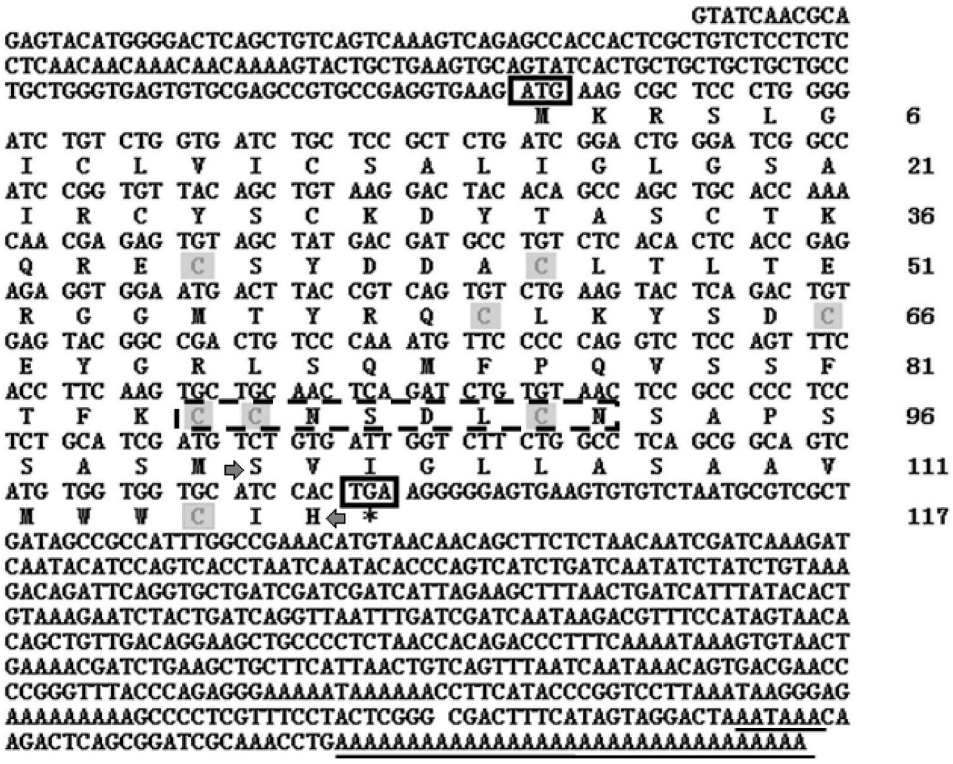

Fig. 1. Nucleotide sequence and deduced amino acid sequence of EcCD59. The initiation codon (ATG) and stop codon (TGA) were boxed, respectively. The potential poly adenylation signal (AATAAA) and the ploy (A) tail were underlined, respectively. The conserved signature motif "CCXXXXCN" was enclosed by a dashed box and conserved cysteine residues were shaded in gray.

proteins were transferred to Bio-Rad PVDF membranes on ice at 100 V for 90 min by using a western blotting system (Bio-Rad, USA). After that, the membranes were washed in TBST for 5 min, incubated with blocking buffer containing 3% BSA for 2 h and then incubated with 1:1000 diluted GST-tag antibody at 4 °C overnight. The PVDF membranes were washed in TBST, incubated with 1:2000 diluted peroxidase-conjugated antibody for 60 min at room temperature. Following 4 times washes in TBST, PVDF membranes were developed and visualized.

2.12. Binding of recombinant EcCD59 or EcCD59delGPI to V. alginolyticus

V. alginolyticus used in this study was cultured until the value of OD_{600} reached approximately 0.8, followed by the resuspension in PBS to 1×10^7 CFU ml^{-1}. ELISA 96-well plates were coated with vibrio suspension at 4 °C overnight, then blocked with 5% milk and washed with 0.5% Tween-20/PBS. After that, various concentrations of the purified GST, EcCD59 or EcCD59delGPI were added to the plates and incubated for 2 h at room temperature, followed by the incubation with *anti*-GST antibody and HRP secondary antibody. Then, 200 µl of TMB diluted in substrate buffer was added and incubated in dark for 30 min. Until the color was developed, 2 M H_2SO_4 was added. The absorbance at 450 nm was determined by a microplate reader [39]. In this study, PBS group was served as negative control and binding index was calculated as follows: OD_{450} nm absorption in text group/OD_{450} nm absorption in negative control group (n = 3).

2.13. Antimicrobial activity

To investigate the effect of EcCD59 on the vibrio growth, the colony-forming unit assay was performed as previous described [24]. In brief, 10 µl of vibrio suspension (2×10^5 CFU ml^{-1}) was incubated with the 2.5 or 50.0 µg of GST, EcCD59, EcCD59delGPI proteins at room temperature for 2 h, followed by 4 times wash with PBS. Then, the mixtures were resuspended and incubated on LB agar plates at 37 °C for 8 h. The experiment was performed in triplicate.

To investigate the effect of EcCD59 on the vibrio growth, the optical density measurement was performed. In brief, 10 µl of vibrio suspension (2×10^5 CFU ml^{-1}) was incubated with the 2.5 or 50.0 µg of GST, EcCD59, EcCD59delGPI proteins at room temperature for 2 h, followed by 4 times wash with PBS. Then, the mixtures were incubated in LB medium in a volume of 10 ml at 37 °C. The absorbance at 600 nm was determined at 4 and 12 h, respectively. The experiment was performed in triplicate.

2.14. In vivo effect of EcCD59 on vibrio infection

To investigate the effect of EcCD59 on the growth of *V. alginolyticus*, the *in vivo* injection was performed as described previously [41]. *V. alginolyticus* was resuspended in PBS, adjusted to 1×10^7 CFU ml^{-1} and incubated with various concentrations of the purified GST, EcCD59 or EcCD59delGPI, respectively. Then, the intraperitoneal injection was performed. In brief, the grouper injected with 2.5 µg GST + vibrio + PBS, 50.0 µg GST + vibrio + PBS, 2.5 µg EcCD59 + vibrio + PBS, 50.0 µg EcCD59 + vibrio + PBS, 2.5 µg EcCD59-delGPI + vibrio + PBS or 50.0 µg EcCD59delGPI + vibrio + PBS was used as GST-2.5 group, GST-50 group, EcCD59–2.5 group, EcCD59-50 group, EcCD59delGPI-2.5 group or EcCD59delGPI-50 group, respectively. The grouper injected with vibrio + PBS was used as the control. 6 fish in each group were collected after 24 h challenge and the samples were preserved in −80 °C. The genomic DNA of the tissues, including the vibrio DNA, was extracted by using a DNA extraction kit (Omega, USA), and the concentration was adjusted to 100 ng/µl qPCR assay was used to detect the gyrB gene of *V. alginolyticus* [42], while the GAPDH gene of grouper was analyzed as the reference gene. The experiments were performed in triplicate.

2.15. Statistical analyses

The data analysis was measured by using SPSS 18 analysis program and represented as means ± standard deviation. All of the experimental data analysis was subjected to one-way ANOVA (one-way analysis of variance). In the further analysis of Duncan's multiple range test, only if the level of P-value < 0.05, the differences were considered

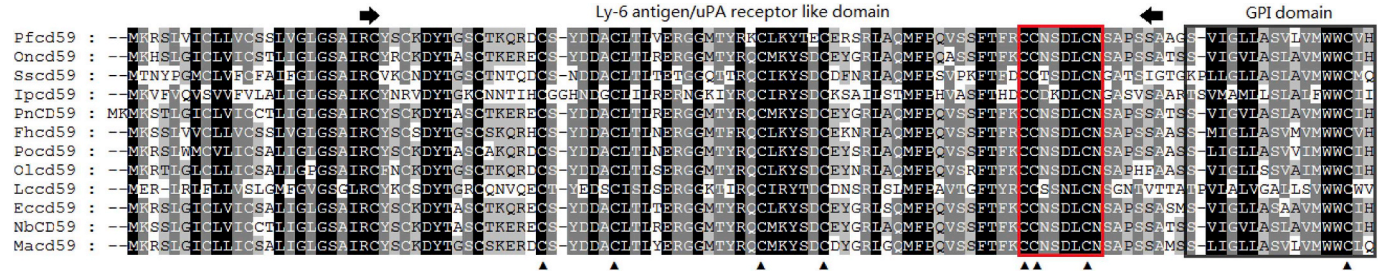

Fig. 2. Multiple sequence alignment of the predicted amino acid sequence of EcCD59 with other CD59 sequences. (PnCD59, *Pundamilia nyererei* CD59, XP_005735060.1); (FhCD59, *Fundulus heteroclitus* CD59, XP_012713747.1); (PfCD59, *Poecilia Formosa* CD59, XP_007540635.1); (OnCD59, *Oreochromis niloticus* CD59, AJB29397.1); (MaCD59, *Monopterus albus* CD59, XP_020474764.1); (PoCD59, *Paralichthys olivaceus* CD59, XP_019966070.1); (OlCD59, *Oryzias latipes* CD59, XP_004086091.1); (SsCD59, *Sus scrofa* CD59, AAC67231.1); (IpCD59, *Ictalurus punctatus* CD59, ABI18969.1); (LcCD59, *Larimichthys crocea* CD59, ABG37787.1); (NbCD59, *Neolamprologus brichardi* CD59, XP_006791961.1). The shared residues represented the similar regions between the different species and the conservative degree was distinguished from light to dark. The Ly-6 antigen/uPA receptor like domain was indicated by arrow and GPI domain was boxed. The signature motif was enclosed in red box and the eight conserved cysteine residues were underlined by black triangle. (For interpretation of the references to color in this figure legend, the reader is referred to the Web version of this article.)

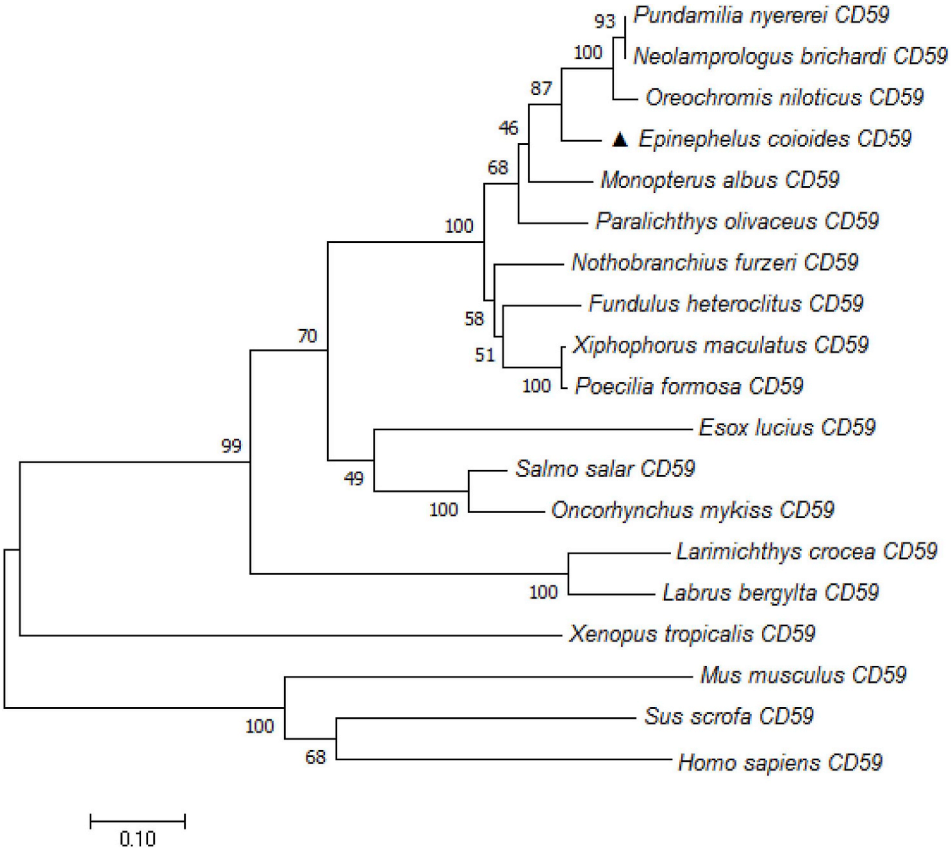

Fig. 3. A phylogenetic tree constructed by using full-length amino acid sequences of CD59. The full-length amino acid sequence of CD59 proteins were extracted from Genbank and analyzed by using Neighbor-Joining method by Mega 6.0 with 1000 bootstrap replications. The numbers shown at branches indicated the bootstrap values (%). Sequence used in analysis with their abbreviation and GenBank accession number: (*Neolamprologus brichardi* CD59, XP_006791961.1); (*Pundamilia nyererei* CD59, XP_005735060.1); (*Oreochromis niloticus* CD59, AJB29397.1); (*Larimichthys crocea* CD59, ABG37787.1); (*Monopterus albus* CD59, XP_020474764.1); (*Paralichthys olivaceus* CD59, XP_019966070.1); (*Fundulus heteroclitus* CD59, XP_012713747.1); (*Poecilia formosa* CD59, XP_007540635.1); (*Xiphophorus maculatus* CD59, XP_005812177.1); (*Nothobranchius furzeri* CD59, XP_015813357.1); (*Esox lucius* CD59, XP_010880289.1); (*Salmo salar* CD59, XP_013981932.1); (*Oncorhynchus mykiss* CD59, NP_001117969.1); (*Xenopus tropicalis* CD59, XP_004913413.1); (*Mus musculus* CD59, AAC00055.1); (*Sus scrofa* CD59, AAC67231.1); (*Homo sapiens* CD59, CAG46523.1); (*Labrus bergylta* CD59, XP_020504540.1).

statistically significant.

3. Results

3.1. Characterization of EcCD59 cDNA sequence

Both complete nucleotide and deduced amino acid sequence of EcCD59 were shown in Fig. 1. Full-length EcCD59 sequence of 1076 bp comprised a 5′UTR of 163 bp, an ORF of 354 bp and a 3′UTR of 559 bp. The nucleotide sequence of EcCD59 predicted a putative polyadenylation signal sequence (AATAAA) at nucleotide 1012, which was 31 bp upstream the poly (A) tail. ORF sequence of EcCD59 encoded a polypeptide of 117 amino acids with an estimated molecular mass of 12.87 KDa and a predicted isoelectric point of 7.88.

In Fig. 2, multiple sequence alignment analysis revealed that EcCD59 was a member of Ly-6 superfamily, containing two functional domains: ly-6 antigen/uPA receptor like domain (amino acids 23–98) and GPI domain (amino acids 101–117). The multiple alignment analysis indicated that the domain structure of EcCD59 was similar to other vertebrate CD59s. Genbank analysis indicated that EcCD59 amino acid sequence exhibited the closest homology to those of *Neolamprologus brichardi* (Accession No. XP006791961.1) with 91% identity, *Pundamilia nyererei* (Accession No. XP005735060.1) with 90% identity and *Oreochromis niloticus* (Accession No.NP001298266.1) with 90% identity. In addition, the predicted EcCD59 amino acid sequence also contained a signal peptide located at amino acids 1–21, while the conserved signature motif “CCXXXXCN” and eight conserved cysteine residues may be involved in formation of disulfide bridges.

Based on the full-length CD59 amino acid sequence, phylogenetic analysis was constructed by using MEGA 6.0 In Fig. 3, EcCD59 sequence

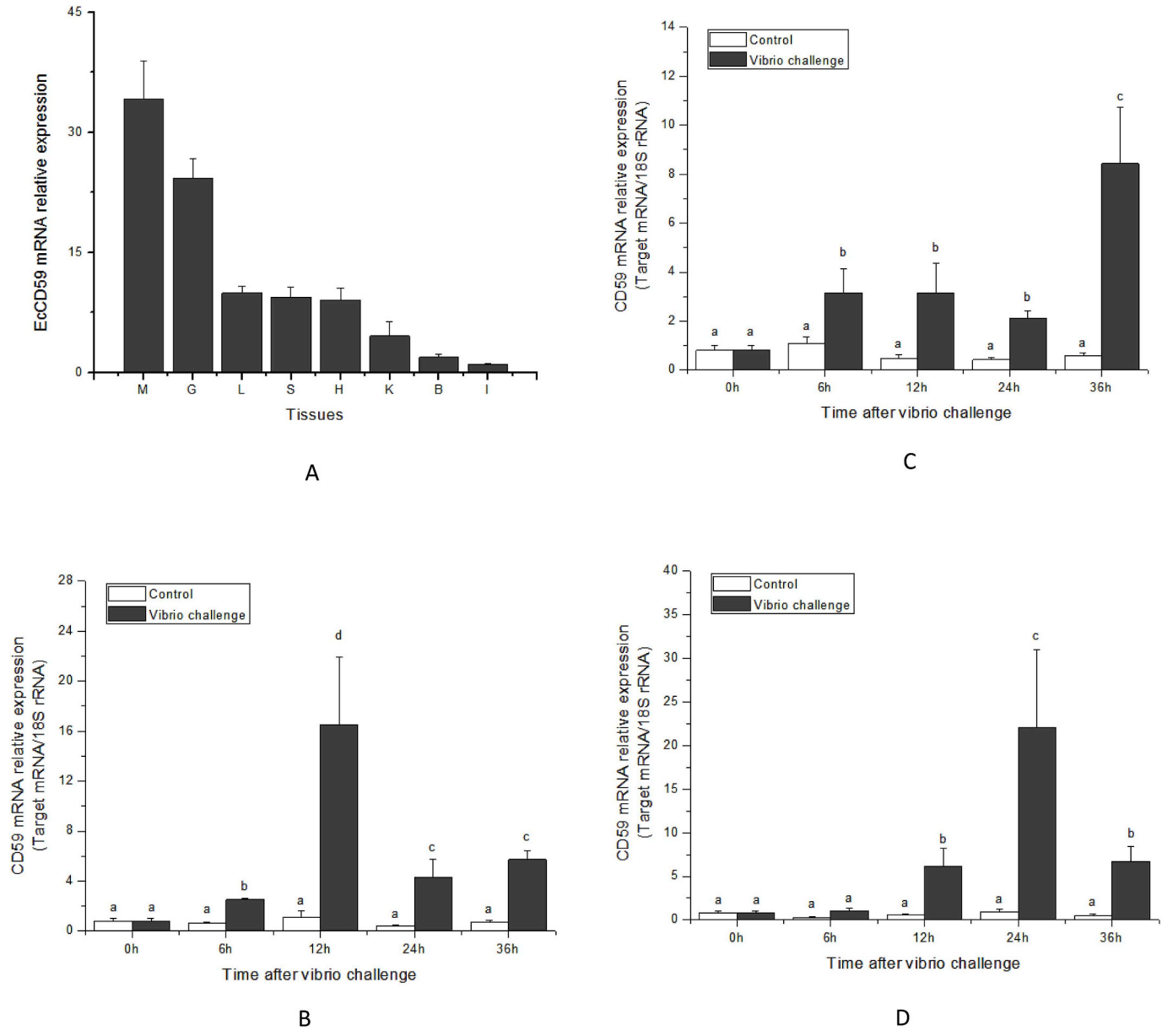

Fig. 4. Gene expression patterns of EcCD59. (A) Tissue-specific mRNA expression of EcCD59 determined by qRT-PCR. The relative EcCD59 transcript expression of each tissue was calculated by the $2^{-\triangle\triangle Ct}$ methods using 18S rRNA as a reference gene, and the relative mRNA level was compared with intestine expression. (B: blood; I: intestine; L: liver; G: gill; S: spleen; H: heart; K: kidney; M: muscle). (B–D) qRT-PCR analysis of EcCD59 mRNA expression in liver, kidney and spleen at 0, 6, 12, 24 and 36 h post-challenge. The calculated data (mean ± SD) of six individuals (n = 6) with different letters were significantly different ($P < 0.05$) between the vibrio challenge group and the control group.

was similar to those of other marine fish *Neolamprologus brichardi*, *Pundamilia nyererei* and *Oreochromis niloticus*. This result of phylogenetic analysis was similar to BLAST results, suggesting that the evolutionary relationship revealed in the phylogenetic trees were in agreement with the concept of the traditional taxonomy.

3.2. Gene expression of EcCD59 mRNA

In Fig. 4A, tissue-specific EcCD59 mRNA expression was detected in all isolated samples (B: blood; I: intestine; L: liver; G: gill; S: spleen; H: heart; K: kidney; M: muscle). A high-level expression of EcCD59 mRNA was observed in muscle, while the lowest expression level was detected in intestine. Moreover, expression patterns of EcCD59 in liver, kidney and spleen were investigated at 0, 6, 12, 24 and 36 h after *V. alginolyticus* challenge. In Fig. 4B, liver EcCD59 mRNA expression increased significantly from 6 h to 36 h and peaked at 12 h post-challenge with the highest value of 16.50-fold greater than that of the control ($P < 0.05$). In Fig. 4C, a sharp increase of EcCD59 mRNA expression in kidney was observed from 6 h to 36 h following *V. alginolyticus* challenge and reached a peaked level at 36 h with the highest value of 14.29-fold greater than that of the control ($P < 0.05$). In Fig. 4D, the elevated level of EcCD59 mRNA expression in spleen began at 12 h post-challenge and peaked at 24 h with the highest value of 23.66-fold greater than that of the control ($P < 0.05$).

3.3. Subcellular localization of EcCD59 in Hela cells

The Subcellular localization of EcCD59 was determined by GFP-EcCD59 fusion protein. In order to characterize the function of GPI domain, we constructed the GPI domain deleted EcCD59 (EcCD59delGPI) ligated to pEGFP-N3 plasmids. As shown in Fig. 5, the green fluorescence signaling was observed throughout cytoplasm and

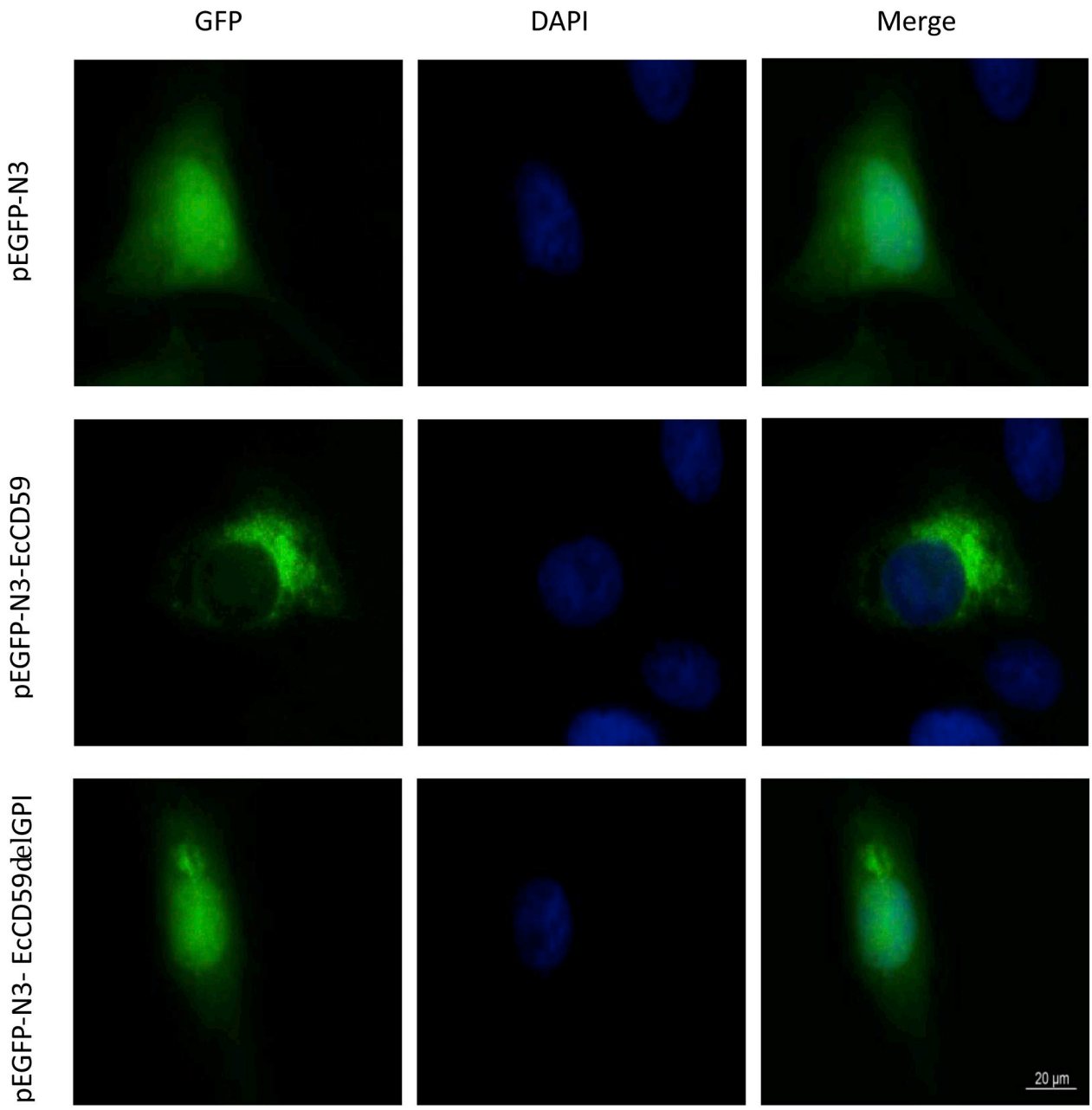

Fig. 5. Subcellular localization of EcCD59 in Hela cells. Cells were transfected with pEGFP-N3 (upper row), pEGFP-N3-EcCD59 (middle row) or pEGFP-N3-EcCD59delGPI (lower row). After allowing the Hela cells to adhere for 24 h in 24-well plates, the nucleus was stained with DAPI and the fluorescence signaling was observed by using fluorescence microscopy.

nucleus in pEGFP-N3 expression cells. In contrast, the green fluorescence signaling was mainly aggregated in cytoplasm in pEGFP-N3-EcCD59 expression cells, while the green fluorescence signaling was observed throughout cytoplasm and nucleus in pEGFP-N3-EcCD59-delGPI expression cells.

3.4. Detection of liver CD59 distribution by immunofluorescence and ELISA assay

As shown in Fig. 6A, the green fluorescence in liver section was predominately colocalized with red fluorescence of membrane probe DiI. In addition, the liver nuclear proteins, cytoplasmic proteins and membrane proteins were isolated for the detection of EcCD59 by ELISA assay. In Fig. 6B, binding index in membrane proteins group was consistently higher among the groups and increased in a dose-dependent manner. These results suggested that EcCD59 should possibly localized in cellular membrane.

3.5. Prokaryotic expression and fusion protein validation

The pGEX4T-2 plasmid, pGEX4T-2-EcCD59 and pGEX4T-2-EcCD59delGPI plasmid were transformed into *E. coli* BL21(DE3) competent cells for protein expression, respectively. After IPTG induction, the whole cell lysates by SDS-PAGE. In Fig.7A, A strong protein band was visualized in pGEX4T-2-EcCD59/EcCD59delGPI transformed cells in comparison with that of pGEX4T-2 transformed cells. Following sonication, the recombinant EcCD59/EcCD59delGPI proteins were purified by using GST bind resin (Millipore). In addition, GST protein was also purified from induced pGEX4T-2 pellets and used as the control. Following the purification, the purified protein GST, EcCD59 and

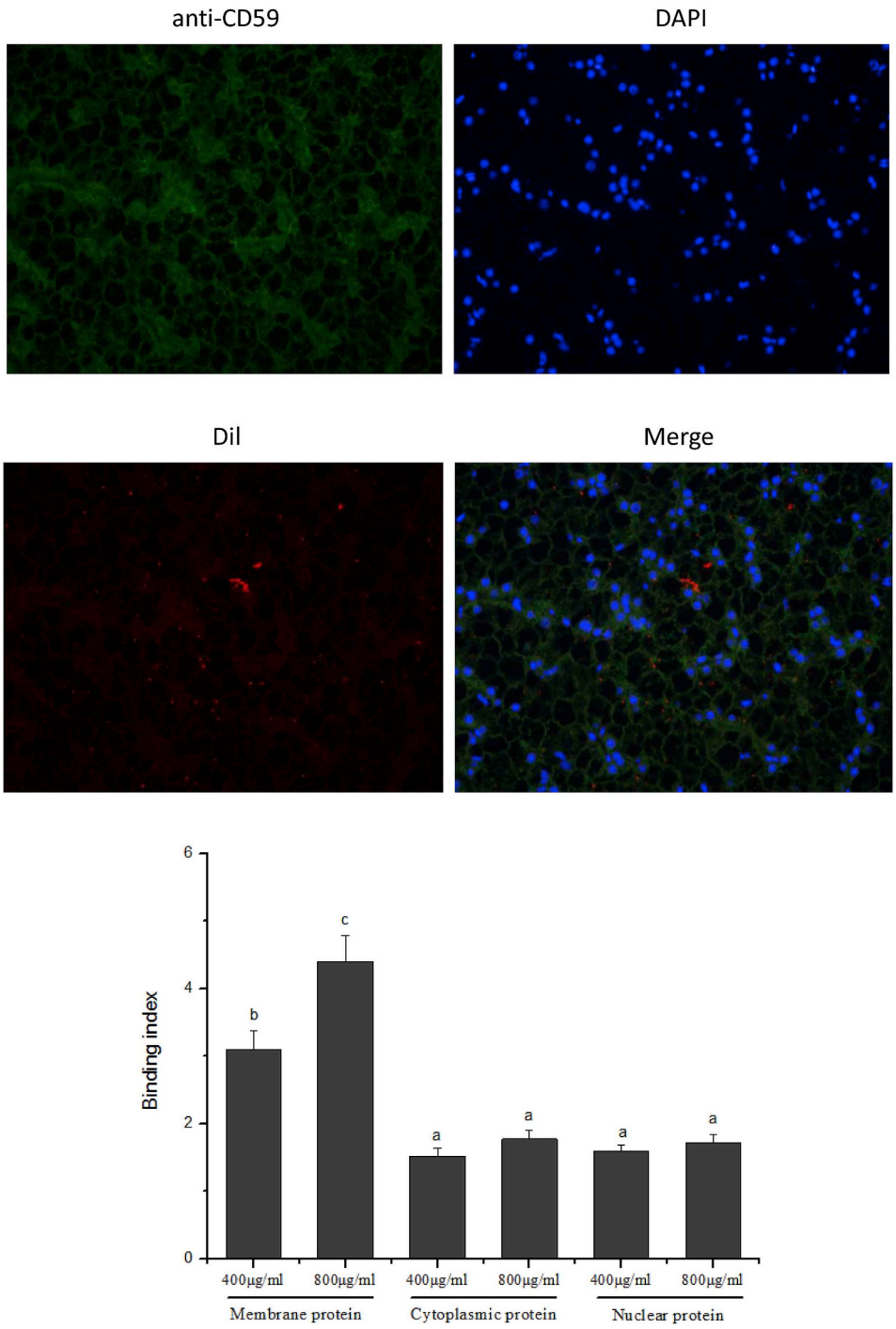

Fig. 6. Detection of CD59 distribution in liver tissues. (A) Immunofluorescence assay. Paraffin-embedded liver sections were incubated with 1:100 diluted anti-CD59 primary antibody (Abcam) overnight at 4 °C. After washing, the slides were incubated with 1:500 diluted FITC-conjugated IgG secondary antibody (Abcam) at room temperature for 1 h. Following washing 3 times with PBS, the slides were incubated with DAPI and membrane probe $DiIC_{18}(3)$ (DiI) for another 20 min. The fluorescence signaling was detected by using a fluorescence microscope (Nikon) (B) ELISA assay. The calculated data (mean ± SD) with different letters were significantly different ($P < 0.05$) among the groups. The experiment was performed in triplicate.

EcCD59delGPI were confirmed by western blotting using *anti*-GST antibody.

3.6. Detection of the binding activity of EcCD59 or EcCD59delGPI to V. alginolyticus

To investigate the possible binding activity of EcCD59 to *V. alginolyticus*, ELISA assay was performed. As shown in Fig. 7B, the binding index in GST group are consistently lower among the groups. In contrast, binding index in EcCD59 group or EcCD59delGPI group increased significantly when the protein concentration increased, implying that EcCD59 or EcCD59delGPI can both directly bind to *V. alginolyticus*.

3.7. Antimicrobial activity of EcCD59 or EcCD59delGPI against V. alginolyticus in vitro

To investigate the possible effect of EcCD59 on the growth of *V. alginolyticus*, the optical density measurement and colony-forming unit assay were performed. As shown in Fig. 8A, the pretreatment with 2.5 μg or 50.0 μg of GST exhibits no inhibitory effect on the growth of *V. alginolyticus* by comparing with that of PBS group, while a decreased OD_{600} value was observed in EcCD59–2.5 group and EcCD59delGPI-2.5 group following 4 h incubation. In contrast, the lowest optical absorption was observed in EcCD59-50 group and EcCD59delGPI-50 group throughout the trial.

In Fig. 8B, *V. alginolyticus* was pretreated with various concentration

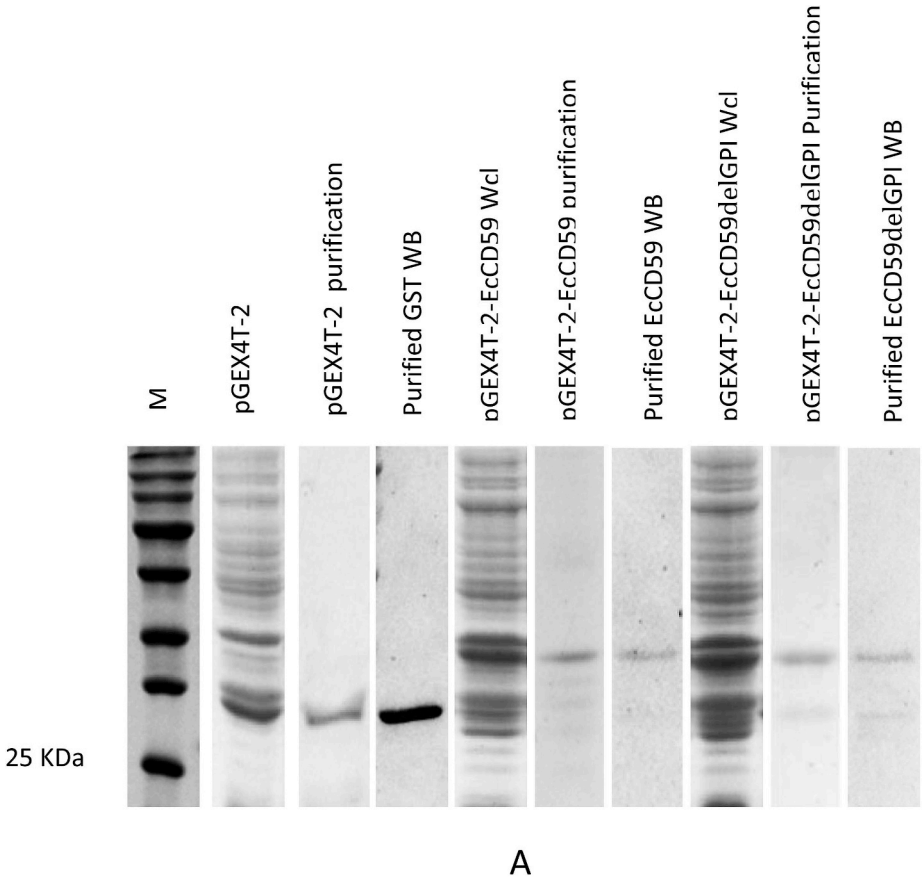

A

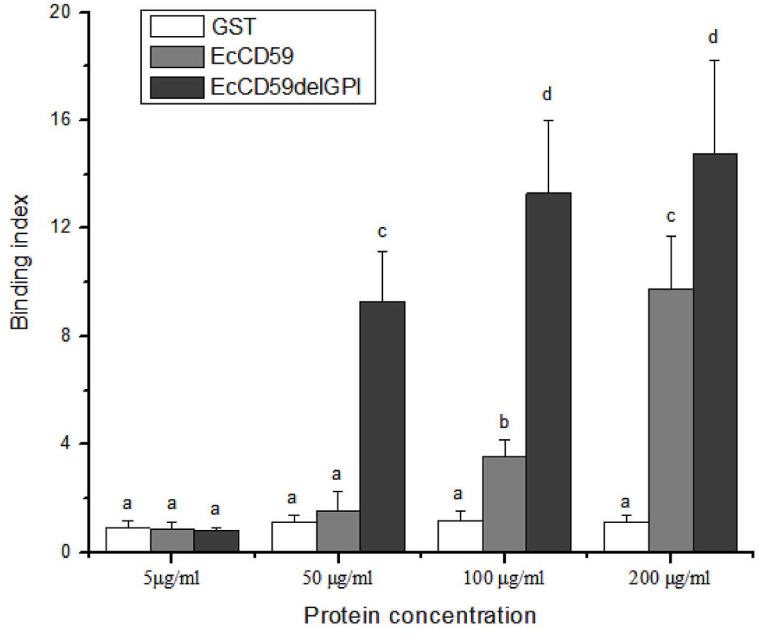

B

Fig. 7. Preparation of recombinant proteins and the detection of their binding activity to *V. alginolyticus*. (A) Production of recombinant EcCD59 and EcCD59delGPI protein. Lane M: Protein molecular standard; Lane pGEX4T-2: Total protein was isolated from the induced pGEX4T-2-BL21; Lane pGEX4T-2 purification: Recombinant GST protein was purified; Lane purified GST WB: Purified recombinant GST protein was identified using *anti*-GST-tag antibody; Lane pGEX4T-2-EcCD59 Wcl: Total protein was isolated from whole cell lysis of the induced pGEX4T-2-EcCD59-BL21; Lane pGEX4T-2-EcCD59 purification: Recombinant pGEX4T-2-EcCD59 protein was purified; Lane pGEX4T-2-EcCD59 WB: Purified recombinant pGEX4T-2-EcCD59 protein was identified using *anti*-GST-tag antibody; Lane pGEX4T-2-EcCD59delGPI Wcl: Total protein was isolated from whole cell lysis of the induced pGEX4T-2-EcCD59delGPI-BL21; Lane pGEX4T-2-EcCD59delGPI purification: Recombinant pGEX4T-2-EcCD59delGPI protein was purified; Lane pGEX4T-2-EcCD59delGPI WB: Purified recombinant pGEX4T-2-EcCD59delGPI protein was identified using *anti*-GST-tag antibody. (B) Determination of the binding activity of EcCD59 or EcCD59delGPI to *V. alginolyticus* by ELISA assay. The calculated data (mean ± SD) with different letters were significantly different ($P < 0.05$) among the groups. The experiment was performed in triplicate.

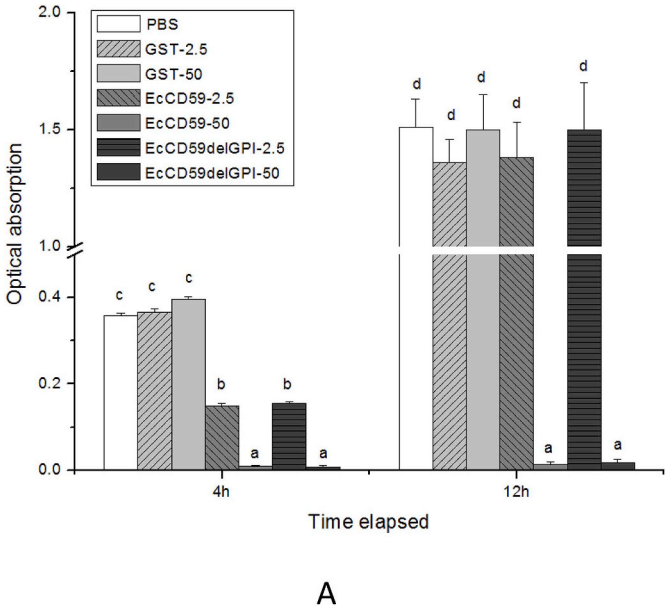

Fig. 8. Determination of antimicrobial activity of EcCD59 or EcCD59delGPI to *V. alginolyticus*.(A) Optical density measurement. The calculated data (mean ± SD) with different letters were significantly different ($P < 0.05$) among the groups. The experiment was performed in triplicate. (B) Colony-forming unit assay. *V. alginolyticus* was incubated with various concentrations of GST, EcCD59 or EcCD59delGPI protein, and then was cultured in LB medium at 37 °C for 8 h, while *V. alginolyticus* incubated in the absence of GST, EcCD59 or EcCD59delGPI protein was used as control. The experiment was performed in triplicate.

of GST, EcCD59 and EcCD59delGPI and then cultured on LB agar medium for another 8 h incubation. In this study, pretreatment with 2.5 μg or 50.0 μg of GST exerts no inhibitory effect on the growth of *V. alginolyticus* by comparing with that of PBS group, while the pre-incubation with 50.0 μg of EcCD59 or EcCD59delGPI can strongly inhibit the growth of *V. alginolyticus in vitro*.

3.8. Inhibitory effect of EcCD59 or EcCD59delGPI on the growth of V. alginolyticus in vivo

The mixtures of *V. alginolyticus* and purified proteins (GST, EcCD59 and EcCD59delGPI) were incubated for 2 h and then was injected intraperitoneally. Following 24 h injection, the vibrio dissemination to kidney and spleen was determined by using qRT-PCR assay. As shown in Fig. 9A and B, the relative expression of *V. alginolyticus* gyrB in kidney and spleen in EcCD59-50 group or EcCD59delGPI-50 group was significantly lower than that of the control, implying that EcCD59 can restrict the growth rate of *V. alginolyticus* and reduce the dissemination behavior of *V. alginolyticus* to kidney and spleen *in vivo*.

4. Discussion

CD59 is a glycoprotein of Ly-6 family containing a conserved motif "CCXXXXCN", which can participate in the inhibition of MAC formation by blocking the incorporation of C9 to C5b-9 assembly [43]. In this study, a high-level expression of EcCD59 mRNA was observed in muscle, while the lowest expression level was detected in intestine. Similarly, a strong expression of muscle CD59 was also detected in zebrafish [11]. Thus, these results indicated that the expression of EcCD59 mRNA was tissue-specific, whereas other tissues may also contribute to its synthesis.

V. alginolyticus, a gram-negative bacteria, can pose a great threat to the survival of marine fish [30]. Liver, kidney and spleen are playing important roles in the teleostean immunity [44]. In this study, we

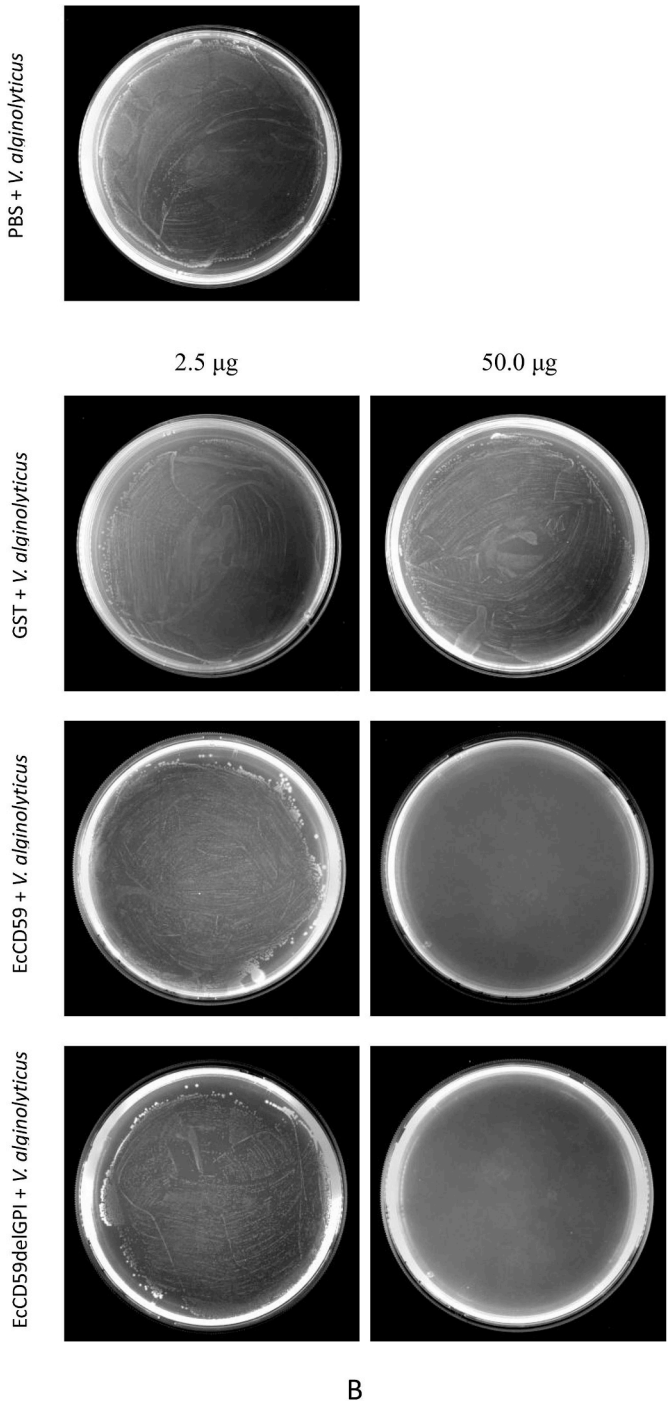

Fig. 8. (*continued*)

investigated the expression patterns of EcCD59 mRNA in the immune-related tissues following *V. alginolyticus* challenge. The up-regulation of CD59 mRNA was observed in liver, kidney and spleen from 6 h to 36 h after *V. alginolyticus* challenge. Similarly, the elevated level of CD59 expression is observed in croaker and Tongue sole following bacterial challenge or poly(I:C) injection [23,24].

Broadly speaking, subcellular localization is an essential characteristic and tightly linked to its function. Increasing evidences indicate that CD59, a membrane-bound protein, contains a conserved GPI motif that can determine its localization and direct to membrane targeting [10]. In this study, the green fluorescence signaling was mainly aggregated in cytoplasm in pEGFP-N3-EcCD59 expression cells, while the green fluorescence signaling was broadly observed in cytoplasm and

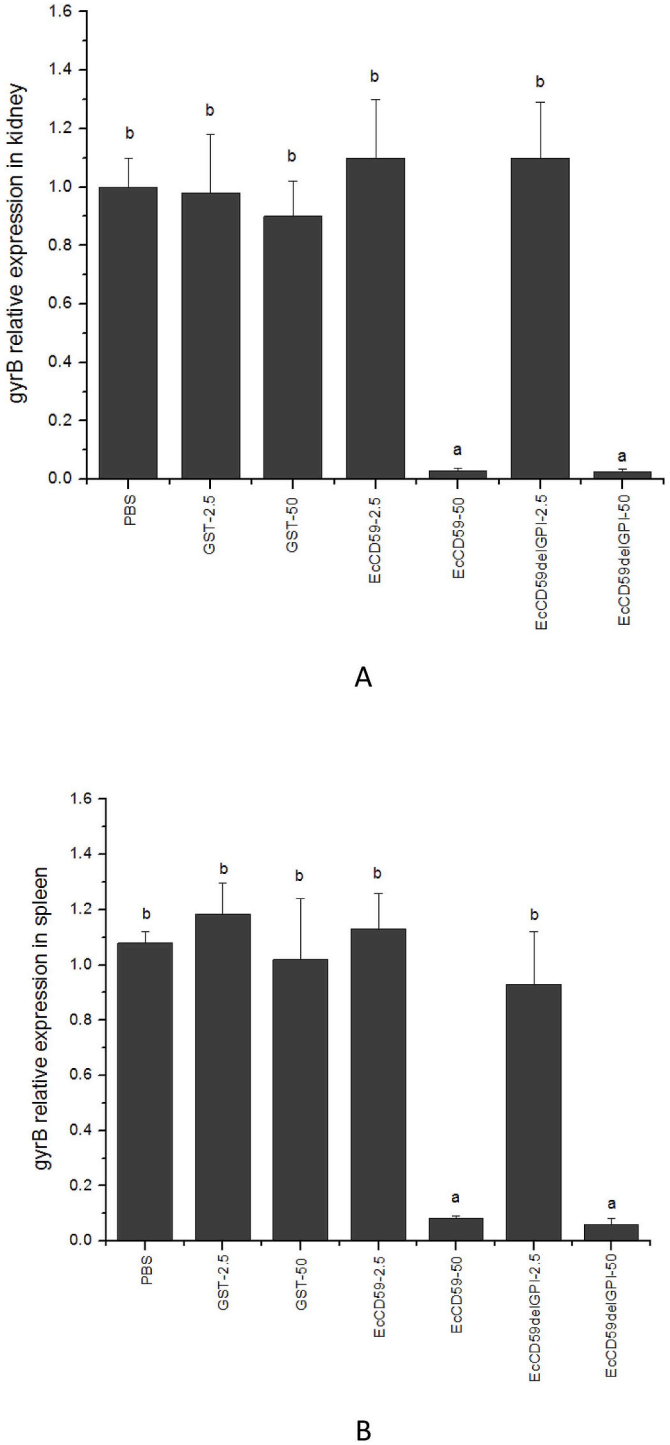

Fig. 9. Inhibitory effect of EcCD59 or EcCD59delGPI on vibrio infection. The mixture of 2.5 μg GST + vibrio + PBS, 50.0 μg GST + vibrio + PBS, 2.5 μg EcCD59 + vibrio + PBS, 50.0 μg EcCD59 + vibrio + PBS, 2.5 μg EcCD59delGPI + vibrio + PBS, 50.0 μg EcCD59delGPI + vibrio + PBS or vibrio + PBS was injected intraperitoneally. Following 24 h injection, the tissue samples were obtained and the total DNA was isolated. Relative expressions of *V. alginolyticus* gyrB in kidney (A) and spleen (B) were determined by qPCR assay. The calculated data (mean ± SD) of six individuals (n = 6) with different letters were significantly different ($P < 0.05$) between the vibrio challenge group and the control group.

nucleus in pEGFP-N3-EcCD59delGPI expression cells, suggesting that the high-conserved GPI motif can determine the subcellular localization of EcCD59 in Hela cells, which was similar to that of mammalian CD59.

Further studies on EcCD59 distribution in liver tissue by immunofluorescence assay indicated that EcCD59 may be possibly predominated in cellular membrane, which was colocalized with red fluorescence signaling of membrane probe Dil. In addition, ELISA assay demonstrated that the isolated membrane proteins showed a higher binding index by comparing to those of nuclear proteins group and cytoplasmic proteins group. These results demonstrated that EcCD59 should be a cellular membrane protein.

As is well known, activated mammalian complement system can elicit a regulatory effect on immune defense system within the host [45], whereas the vicinity of a hydrophobic groove and N-linked glycosylation in mammalian CD59 are active sites, which can disrupt C9 insertion and polymerization, thus preventing the occurrence of complement-dependent lysis and proinflammatory activity [46]. *E. coli* can resist the *in vivo* killing mechanism of complement cascades by directly binding to human cell membrane-released CD59 [47]. In fish, accumulating evidences demonstrated that the recombinant LycCD59 protein can exert a species-selective inhibitory activity on complement cascades and antagonize the complement-dependent erythrocyte lysis *in vitro* [23]. However, CD59 may play a complex role in teleostean immunity following bacterial infection. Previous findings indicated that recombinant Tongue sole CD59 protein can facilitate invading bacteria to escape complement-mediated killing mechanism *in vitro* [24], whereas both recombinant zebrafish CD59 or OnCD59 proteins can exhibit a novel function in teleostean immune defense against bacterial infection, which can not only exhibit a direct binding activity to LPS, LTA and bacteria, but also restrict bacterial growth in a complement-independent manner [11,22]. However, the mechanism linking grouper CD59 to teleostean immunity is still unclear. Thus, we obtained purified recombinant EcCD59 and EcCD59delGPI protein to investigate its possible function in immunity. In this study, ELISA assay demonstrated that both EcCD59 and EcCD59delGPI can directly bind to *V. alginolyticus*. In addition, the pretreatment with EcCD59 or EcCD59delGPI can restrict growth of *V. alginolyticus in vitro* and decrease its dissemination to kidney and spleen *in vivo*. Taken together, we predicted that EcCD59 or EcCD59delGPI can restrict growth of *V. alginolyticus* and inhibit its invasive behavior *in vivo* by directly binding to *V. alginolyticus*, while loss of GPI domain cannot hamper its inhibitory effect. However, the molecular mechanism underlying inhibitory effect of EcCD59 may require further study.

In summary, we firstly cloned and characterized EcCD59 cDNA and investigated up-regulation of EcCD59 mRNA expression after *V. alginolyticus* challenge. Both recombinant EcCD59 and EcCD59delGPI proteins can directly bind to *V. alginolyticus in vitro*. The administration of EcCD59 and EcCD59delGPI can restrict growth of *V. alginolyticus in vitro and in vivo*. Moreover, GPI domain in EcCD59 plays a key role in the determining its subcellular localization, whereas loss of GPI domain cannot restrict its vibrio-binding and vibrio-inhibitory activity. Our results indicated that EcCD59 may play a regulatory role in immunity in a complement-independent manner.

Acknowledgements

This project was supported by Guangzhou science and technology plan project (grant nos. 201707010135) and National Natural Science Foundation of China (Grant No.31670423).

References

[1] H.J. Muller-Eberhard, The membrane attack complex of complement, Annu. Rev. Immunol. 4 (1) (1986) 503–528.

[2] H.L. Collins, G.J. Bancroft, Cytokine enhancement of complement-dependent phagocytosis by macrophages: synergy of tumor necrosis factor-α and granulocyte--macrophage colony-stimulating factor for phagocytosis of Cryptococcus neoformans, Eur. J. Immunol. 22 (6) (1992) 1447–1454.

[3] L.S. Schlesinger, C.G. Bellinger-Kawahara, N.R. Payne, M.A. Horwitz, Phagocytosis of Mycobacterium tuberculosis is mediated by human monocyte complement

receptors and complement component C3, J. Immunol. 144 (7) (1990) 2771–2780.
[4] I. Goldstein, D. Roos, H. Kaplan, G. Weissmann, Complement and immunoglobulins stimulate superoxide production by human leukocytes independently of phagocytosis, J. Clin. Investig. 56 (5) (1975) 1155.
[5] B.P. Morgan, K.J. Marchbank, M.P. Longhi, C.L. Harris, A.M. Gallimore, Complement: central to innate immunity and bridging to adaptive responses, Immunol. Lett. 97 (2) (2005) 171–179.
[6] A. Sahu, J.D. Lambris, Structure and biology of complement protein C3, a connecting link between innate and acquired immunity, Immunol. Rev. 180 (1) (2001) 35–48.
[7] C. Liang-Takasaki, H. Saxen, P. Mäkelä, L. Leive, Complement activation by polysaccharide of lipopolysaccharide: an important virulence determinant of salmonellae, Infect. Immun. 41 (2) (1983) 563–569.
[8] B.P. Morgan, M.J. Walport, Complement deficiency and disease, Immunol. today 12 (9) (1991) 301–306.
[9] A.D. Papanastasiou, E. Georgaka, I.K. Zarkadis, Cloning of a CD59-like gene in rainbow trout: expression and phylogenetic analysis of two isoforms, Mol. Immunol. 44 (6) (2007) 1300–1306.
[10] A. Davies, P.J. Lachmann, Membrane defence against complement lysis: the structure and biological properties of CD59, Immunol. Res. 12 (3) (1993) 258.
[11] C. Sun, J. Wu, S. Liu, H. Li, S. Zhang, Zebrafish CD59 has both bacterial-binding and inhibiting activities, Dev. Comp. Immunol. 41 (2) (2013) 178–188.
[12] J. Petranka, J. Zhao, J. Norris, N.B. Tweedy, R.E. Ware, P.J. Sims, et al., Structure-function relationships of the complement regulatory protein, CD59, Blood Cells Mol. Dis. 22 (3) (1996) 281–296.
[13] S.A. Rollins, P. Sims, The complement-inhibitory activity of CD59 resides in its capacity to block incorporation of C9 into membrane C5b-9, J. Immunol. 144 (9) (1990) 3478–3483.
[14] S.A. Rollins, J. Zhao, H. Ninomiya, P. Sims, Inhibition of homologous complement by CD59 is mediated by a species-selective recognition conferred through binding to C8 within C5b-8 or C9 within C5b-9, J. Immunol. 146 (7) (1991) 2345–2351.
[15] P.E. Korty, C. Brando, E.M. Shevach, CD59 functions as a signal-transducing molecule for human T cell activation, J. Immunol. 146 (12) (1991) 4092–4098.
[16] U. Krus, B.C. King, V. Nagaraj, N.R. Gandasi, J. Sjölander, P. Buda, et al., The complement inhibitor CD59 regulates insulin secretion by modulating exocytotic events, Cell Metabol. 19 (5) (2014) 883–890.
[17] S. Chen, T. Caragine, N.-K.V. Cheung, S. Tomlinson, CD59 expressed on a tumor cell surface modulates decay-accelerating factor expression and enhances tumor growth in a rat model of human neuroblastoma, Cancer Res. 60 (11) (2000) 3013–3018.
[18] B. Magnadóttir, Innate immunity of fish (overview), Fish Shellfish Immunol. 20 (2) (2006) 137–151.
[19] M. Nonaka, S.L. Smith, Complement system of bony and cartilaginous fish, Fish Shellfish Immunol. 10 (3) (2000) 215–228.
[20] M.C.H. Holland, J.D. Lambris, The complement system in teleosts, Fish Shellfish Immunol. 12 (5) (2002) 399–420.
[21] S. Luo, F. Xie, Y. Liu, W.-N. Wang, Molecular cloning, characterization and expression analysis of complement component C8 beta in the orange-spotted grouper (Epinephelus coioides) after the Vibrio alginolyticus challenge, Gene 558 (2) (2015) 291–298.
[22] Z. Gan, B. Wang, W. Zhou, Y. Lu, W. Zhu, J. Tang, et al., Molecular and functional characterization of CD59 from Nile tilapia (Oreochromis niloticus) involved in the immune response to Streptococcus agalactiae, Fish Shellfish Immunol. 44 (1) (2015) 50–59.
[23] G. Liu, J. Zhang, X. Chen, Molecular and functional characterization of a CD59 analogue from large yellow croaker Pseudosciana crocea, Mol. Immunol. 44 (15) (2007) 3661–3671.
[24] Z.H. Sui, M.F. Li, L. Sun, Tongue sole (Cynoglossus semilaevis) CD59: a complement inhibitor that binds bacterial cells and promotes bacterial escape from the killing of fish serum, Fish Shellfish Immunol. 58 (2016) 442–448.
[25] R.R. Colwell, Global climate and infectious disease: the cholera paradigm*, Science 274 (5295) (1996) 2025–2031.
[26] J. Martinez-Urtaza, J.C. Bowers, J. Trinanes, A. DePaola, Climate anomalies and the increasing risk of Vibrio parahaemolyticus and Vibrio vulnificus illnesses, Food Res. Int. 43 (7) (2010) 1780–1790.
[27] C. Baker-Austin, J.A. Trinanes, N.G. Taylor, R. Hartnell, A. Siitonen, J. Martinez-Urtaza, Emerging Vibrio risk at high latitudes in response to ocean warming, Nat. Clim. Change 3 (1) (2013) 73–77.
[28] T.J. Bowden, Modulation of the immune system of fish by their environment, Fish Shellfish Immunol. 25 (4) (2008) 373–383.
[29] R. Harikrishnan, C. Balasundaram, M.-S. Heo, Molecular studies, disease status and prophylactic measures in grouper aquaculture: economic importance, diseases and immunology, Aquaculture 309 (1) (2010) 1–14.
[30] K.-K. Lee, Pathogenesis studies on Vibrio alginolyticus in the grouper, Epinephelus malabaricus, Bloch et Schneider, Microb. Pathog. 19 (1) (1995) 39–48.
[31] E.A. Ganesh, S. Das, K. Chandrasekar, G. Arun, S. Balamurugan, Monitoring of total heterotrophic bacteria and Vibrio spp. in an aquaculture pond, Curr. Res. J. Biol. Sci. 2 (1) (2010) 48–52.
[32] Q. Wang, Q. Liu, X. Cao, M. Yang, Y. Zhang, Characterization of two TonB systems in marine fish pathogen Vibrio alginolyticus: their roles in iron utilization and virulence, Arch. Microbiol. 190 (5) (2008) 595–603.
[33] K.-C. Yii, T.-I. Yang, K.-K. Lee, Isolation and characterization of Vibrio carchariae, a causative agent of gastroenteritis in the groupers, Epinephelus coioides, Curr. Microbiol. 35 (2) (1997) 109–115.
[34] S. Luo, Y. Huang, F. Xie, X. Huang, Y. Liu, W. Wang, et al., Molecular cloning, characterization and expression analysis of PPAR gamma in the orange-spotted grouper (Epinephelus coioides) after the Vibrio alginolyticus challenge, Fish Shellfish Immunol. 43 (2) (2015) 310–324.
[35] S.-W. Luo, W.-N. Wang, R.-C. Xie, F.-X. Xie, J.-R. Kong, Y.-C. Xiao, et al., Molecular cloning and characterization of PTEN in the orange-spotted grouper (Epinephelus coioides), Fish Shellfish Immunol. 58 (2016) 686–700.
[36] S.-W. Luo, L. Cai, Z.-H. Qi, C. Wang, Y. Liu, W.-N. Wang, Effects of a recombinant complement component C3b functional fragment α 2 MR (α 2-macroglobulin receptor) additive on the immune response of juvenile orange-spotted grouper (Epinephelus coioides) after the exposure to cold shock challenge, Fish Shellfish Immunol. 45 (2) (2015) 346–356.
[37] S.-W. Luo, W.-N. Wang, Z.-M. Sun, F.-X. Xie, J.-R. Kong, Y. Liu, et al., Molecular cloning, characterization and expression analysis of (B-cell lymphoma-2 associated X protein) Bax in the orange-spotted grouper (Epinephelus coioides) after the Vibrio alginolyticus challenge, Dev. Comp. Immunol. 60 (2016) 66–79.
[38] Q. Liang, X. Wu, P. Yang, J. Kong, W. Wei, X. Qiao, et al., The role of delta-1-pyrroline-5-carboxylate dehydrogenase (P5CDh) in the Pacific white shrimp (Litopenaeus vannamei) during biotic and abiotic stress, Aquat. Toxicol. 208 (2019) 1–11.
[39] S.-W. Luo, H. Kang, R.-C. Xie, W. Wei, Q-j Liang, Y. Liu, et al., N-terminal domain of EcC1INH in Epinephelus coioides can antagonize the LPS-stimulated inflammatory response, Fish Shellfish Immunol. 84 (2019) 8–19.
[40] S.-W. Luo, H. Kang, J.-R. Kong, R.-C. Xie, Y. Liu, W.-N. Wang, et al., Molecular cloning, characterization and expression analysis of (B-cell lymphoma-2) Bcl-2 in the orange-spotted grouper (Epinephelus coioides), Dev. Comp. Immunol. 76 (2017) 150–162.
[41] L. Wang, C. Fan, W. Xu, Y. Zhang, Z. Dong, J. Xiang, et al., Characterization and functional analysis of a novel C1q-domain-containing protein in Japanese flounder (Paralichthys olivaceus), Dev. Comp. Immunol. 67 (2016).
[42] P. Luo, C. Hu, Vibrio alginolyticus gyrB sequence analysis and gyrB-targeted PCR identification in environmental isolates, Dis. Aquat. Org. 82 (3) (2008) 209–216.
[43] Y. Huang, F. Qiao, R. Abagyan, S. Hazard, S. Tomlinson, Defining the CD59-C9 binding interaction, Mol. Immunol. 44 (1) (2007) 187-187.
[44] C.M. Press, Ø. Evensen, The morphology of the immune system in teleost fishes, Fish Shellfish Immunol. 9 (4) (1999) 309–318.
[45] K. Joiner, E. Brown, M. Frank, Complement and bacteria: chemistry and biology in host defense, Annu. Rev. Immunol. 2 (1) (1984) 461–492.
[46] J. Yu, R. Abagyan, S. Dong, A. Gilbert, V. Nussenzweig, S. Tomlinson, Mapping the active site of CD59, J. Exp. Med. 185 (4) (1997) 745–754.
[47] R. Rautemaa, G. Jarvis, P. Marnila, S. Meri, Acquired resistance of Escherichia coli to complement lysis by binding of glycophosphoinositol-anchored protectin (CD59), Infect. Immun. 66 (5) (1998) 1928–1933.